

Article

Evaluating the Efficiency of Surface-Based Air Heating Systems

Slawomir Rabczak *  and Krzysztof Nowak 

Faculty of Civil and Environmental and Architecture, Rzeszow University of Technology, 35-959 Rzeszow, Poland; krzynow@prz.edu.pl

* Correspondence: rabczak@prz.edu.pl

Abstract: This study explores the synergistic potential of integrating forced air heating with flat surface heating, presenting a promising solution for structures with intermittent occupancy or where conventional water-based heating proves impractical. The objective is to enhance thermal comfort and reduce long-term energy consumption. A comprehensive examination of the interaction between heated surfaces and forced air heating reveals that excess energy generated can be redirected for more efficient heat distribution. Various scenarios were tested, indicating that the power necessary for maintaining consistent surface temperature could be significantly reduced. A noteworthy approach involves utilizing heat from pellet smoke to maximize heat recovery efficiency from pellet combustion. This, however, raises issues related to smoke introduction into heated spaces. Despite challenges, this approach provides a means to minimize the delivery of overheated air and accumulate energy within room partitions, thereby enhancing system efficiency. The study concludes that while the stand-alone flat surface heating system is better suited as a supplementary heating source within buildings, it offers a compelling alternative within traditional construction, aligning with historical systems.

Keywords: heating integration; energy efficiency; forced air systems



Citation: Rabczak, S.; Nowak, K. Evaluating the Efficiency of Surface-Based Air Heating Systems. *Energies* **2024**, *17*, 1252. <https://doi.org/10.3390/en17051252>

Academic Editors: Leonardo Primavera and Eliseu Monteiro

Received: 31 January 2024
Revised: 19 February 2024
Accepted: 29 February 2024
Published: 6 March 2024



Copyright: © 2024 by the authors. Licensee MDPI, Basel, Switzerland. This article is an open access article distributed under the terms and conditions of the Creative Commons Attribution (CC BY) license (<https://creativecommons.org/licenses/by/4.0/>).

1. Introduction

The hypocaustum was a heating system utilized in ancient times, particularly within the Roman culture, in buildings such as bathhouses, pools, market halls, mausoleums, and wealthy Roman homes, as well as across European cultures. The hypocaustum system consisted of a network of pipes or channels placed beneath the floor or within walls through which a stream of hot air or water flowed, resulting in the heating of indoor spaces [1–3].

Initially, the hypocaustum system comprised torches that were burned beneath the floor. In later periods, these were replaced with channels through which hot air flowed. During the Roman Empire, the hypocaustum system was well developed, with air being heated by furnaces and then directed through channels beneath the floor.

One of the greatest achievements in Roman engineering was the use of the hypocaustum in public bathhouses. In this system, not only the floor but also the walls were heated, providing well-ventilated and heated spaces. In some bathhouses, the hypocaustum was so sophisticated that it provided different temperature levels in various parts of the building [4–6].

To construct a hypocaustum system, proper groundwork was essential. Stone slabs or bricks were first laid on the ground, followed by the creation of a network of channels for hot air or water to pass through. Additional slabs or bricks were placed on top, and the floor or walls were then constructed. This concealed the hypocaustum system while ensuring effective heating [7–9].

The hypocaustum system was employed in various forms by many cultures and civilizations worldwide. In ancient Egypt, systems similar to the Roman hypocaustum were used but in a different form that utilized hot water instead of air. Similar systems were also used in China, Greece, and pre-Columbian cultures in South America [10–12].

Today, the hypocaustum serves as inspiration for modern heating systems, especially in the case of underfloor heating systems, where pipes with hot water or air are placed within the floor. However, modern underfloor heating systems employ more advanced technologies such as electric heat pumps [10,13–16]. Moreover, in the literature, there are many references to surface cooling using both heat pumps [17,18] and renewable sources [19–22].

In this publication, we present the results of an experiment aimed at determining the heating capacity of a plate with specified dimensions supplied with warm air, as well as defining its basic parameters, such as surface temperature under changing thermal load conditions and heat transfer efficiency. In the studied case, an electric heater was used as the heat source. The experiment's goal is also to determine how different thermal load conditions affect the efficiency of the plate heated by warm air. This study may help identify the optimal conditions for utilizing this heating technology and assess its advantages and disadvantages in comparison to traditional heating systems. The research objective is to determine the efficiency of the heating plate depending on the heat supply system: electric heater, 100% air recirculation with an electric heater, and smoke from pellet combustion as a heat source for surface heating. Currently, there are no detailed data on the effectiveness of this type of system, which constitutes a gap in this area.

The basics of the hypocaustum system are presented in the work of Barba, S. and Bansal, N.K. describing existing solutions in the analyzed scope and characteristic parameters of the system [4,5]. However, the work does not include the case of a heating plate with several channels through which heated air or exhaust gases flow. The issue of energy efficiency in older buildings with an air heating system was discussed in the publications of Theis, C. and Lidelöw, S. [7,8]; however, the theoretical considerations concerned the case of forced air heating. To some extent, the topics discussed in this study were covered in the publications of Basaran, T. from 1998 [11]; however, the system concerned heating water in baths, while the system discussed by the authors concerns directly heating the air in the room through convection and radiation. For this reason, the work constitutes a new approach to determining the energy efficiency of the analyzed heating plate using heated air as a heat carrier.

During the literature review of the analyzed issue, we also focused on conducting bibliometric analysis. Through this method, we sought to identify and assess significant scientific publications and their impact in the area of our study. Bibliometric analysis allowed us to gain a deeper understanding of the structure and dynamics of the field, considering citation counts, impact factors, and collaboration networks among researchers, which constituted a significant aspect of our research approach.

Bibliometric analysis is a research method that uses statistical tools to collect, process, and analyze bibliographic information from scientific publications. Its main goal is to assess the impact of these publications on the development of a specific field of science and to identify key authors, journals, topics, and research institutions.

To carry out the analysis, CiteSpace 6.3.R1 software developed by Chaomei Chen was used, which enables the analysis of publications and citations while generating visual representations that illustrate the interrelationships between publications, authors, institutions, and keywords [23–25].

In this study, data were taken from the Web of Science database using the search term “Warm air heating”. Filters were then applied, focusing on issues related to ventilation systems and building construction. The total number of publications for bibliometric analysis is 11,243.

Table 1 presents the 10 universities with the highest centrality index, which is a key aspect of the analysis. The centrality index allows for the identification of nodes that constitute key connections between different research groups. The node with the highest centrality index is usually an institution characterized by innovation and frequent citation by other scientists, which proves its importance in scientific research in a given area.

Table 1. Top 10 institutes with the highest centrality index.

Institution	Number of Publications	Centrality
Technical University of Denmark	195	0.11
United States Department of Energy	274	0.11
Tsinghua University	313	0.08
University of London	66	0.06
UDICE—French Research Universities	119	0.06
Centre national de la recherche scientifique	154	0.06
Yonsei University	32	0.05
Hunan University	181	0.05
National University of Singapore	68	0.04
Lawrence Berkeley National Laboratory	121	0.04

The analysis shows that the Technical University of Denmark and the United States Department of Energy play a key role in the field of warm air heating research due to their high centrality index. This means that these institutions are central players in the study of this topic and enjoy the highest respect in the scientific community. It follows that the works of scientists from these universities are often cited in the scientific literature, which proves their importance in developing knowledge in the field of renewable energy sources. The number of publications does not always correlate with the level of citations. This suggests that there are certain factors, such as research quality and innovation, that influence whether research papers will be noticed and cited by other scientists. It is worth emphasizing that a high centrality index does not necessarily mean a large number of publications but rather a significant impact on the development of knowledge in a given field.

2. Materials and Methods

In this study, a research experiment was conducted with the primary aim of determining the heating efficiency of a plate depending on the airflow rate and the temperature of air passing through channels embedded in a concrete plate. Two operating scenarios were analyzed. The first one pertained to forced air surface heating without recirculation, where the heat source was an electric heater. The second scenario involved forced air surface heating with recirculation, also utilizing an electric heater as the heat source. The third scenario used smoke from pellet combustion to heat the mock-up. Block diagrams illustrating the analyzed solutions are presented in Figures 1–3.

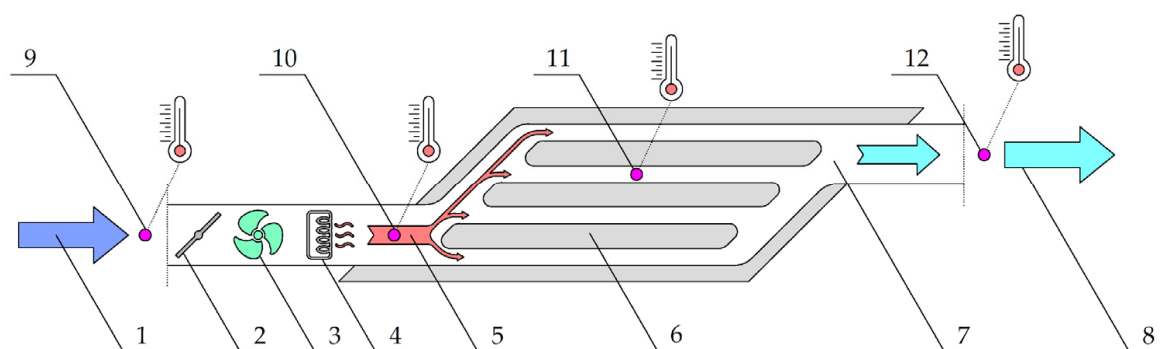


Figure 1. Diagram of surface air heating without recirculation: 1—outdoor air, 2—throttle, 3—fan, 4—electric heater, 5—air collector, 6—mock-up of surface heating, 7—air collector, 8—exhaust of air outside, 9—measurement of initial temperature and airflow, 10—thermostat and measurement of temperature, 11, 12—measurement of temperature.

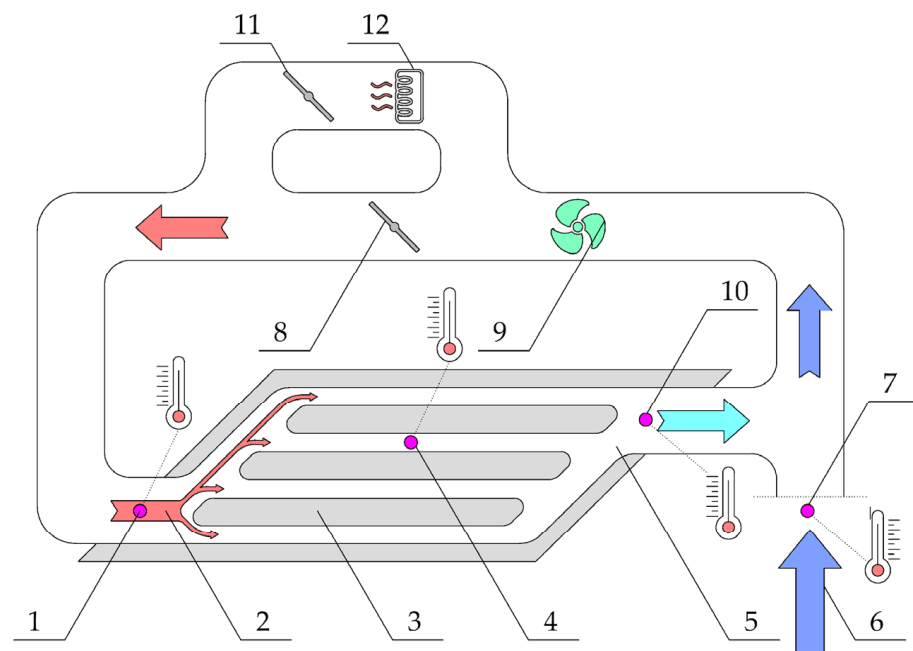


Figure 2. Diagram of surface air heating with recirculation: 1—measurement of temperature, 2—air collector, 3—mock-up of surface heating, 4—measurement of temperature, 5—air collector, 6—outdoor air, 7—measurement of initial temperature and airflow, 8—throttle, 9—fan, 10—measurement of temperature, 11—throttle, 12—electric heater.

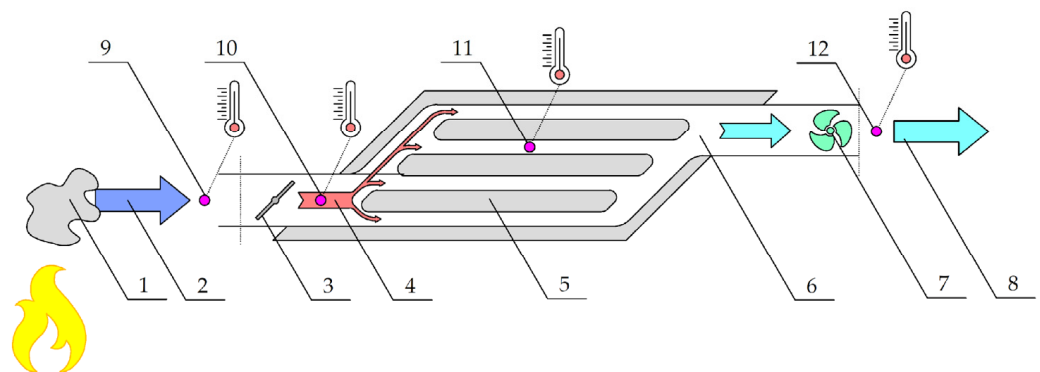


Figure 3. Block diagram of heating by means of flue gas from a pellet-fired boiler: 1—pellet fireplace, 2—smoke from burning pellets, 3—throttle, 4—air collector, 5—mock-up of surface heating, 6—air collector, 7—fan, 8—exhaust of air outside, 9—measurement of initial temperature and airflow, 10—thermostat and measurement of temperature, 11, 12—measurement of temperature.

To conduct the experiment, a model of an underfloor heating system was employed, consisting of 50 mm diameter channels made from thin PVC pipes. The concrete layer in which the channels were placed could be constructed as a prefabricated element or customized for specific orders.

As part of the experiment's preparation, a mock-up of the surface heating system was built, representing a section of a larger potentially heated area. The mock-up took the form of an underfloor heating model measuring $0.5 \times 2 \times 0.3$ m. The layered structure included, from the bottom up: a stabilizing underlay of 5 cm (concrete with polypropylene additive, thermal conductivity coefficient $\lambda = 1.65$ W/mK), a 10 cm thermal insulation layer composed of Styrofoam (thermal conductivity coefficient $\lambda = 0.037$ W/mK), a 0.2 mm thick aluminum foil layer, PVC pipes with a 50 mm diameter (thermal conductivity coefficient $\lambda = 0.170$ W/mK), and a 15 cm concrete screed (thermal conductivity coefficient $\lambda = 1.00$ W/mK). The total heat transfer coefficient in the upward direction was

$U = 0.321 \text{ W/m}^2\text{K}$. The heating pipes are laid with a slope of 1.5‰ to drain any moisture. The mock-up allowed the experiment to be conducted in two variations: one without air recirculation and one with recirculation.

The experiment took place in a thermally insulated single-story technical building with a ground-level floor. All openings in the external walls were sealed against uncontrolled airflow and excessive heat loss. The room measured $3.4 \times 4 \text{ m}$ in plan and had a height of 3.2 m. It should be noted that the building was thermally insulated, but it is difficult to state unequivocally that the measurement system did not lose heat to the surroundings or outside the building's thermal envelope. This may be evidenced by the achievement of stabilized temperatures in the measurement system, which could balance heat losses through the building's thermal shield. Moreover, it should be assumed that there were heat losses through the lower part of the slab (despite the polystyrene insulation), as well as losses on the ducts supplying warm air to the model.

In addition to the mock-up itself, placed on a support structure made of steel profiles at a height of approximately 1.2 m above the floor, the experimental setup included an axial fan connected on the discharge side of the heating plate, an electric heater with modulated power up to 2000 W, set on 500 W during the experiment, and a temperature measurement system with thermometers in the range of -20 to $50 \text{ }^\circ\text{C}$ with an accuracy of 0.5 K. According to energy balance, the power delivered by the airflow (dq_d) should be completely transferred to the room air, which suggests that dq_p should be equal to dq_d unless there is some heat loss. At the same time, we would like to point out that the slab is made of concrete, the heat capacity of which is very high, i.e., approx. 0.92 kJ/kgK . The concrete model itself weighs (excluding Styrofoam and pipes) 440 kg, which allows it to accumulate heat in the amount of 407 kJ/K. Therefore, the stabilization stage lasted from 5 to 13 min, depending on the variant. After this stage of heat accumulation in concrete, the amount of heat supplied and released should be the same. The only heat losses that occurred in the system were losses on the pipes supplying heat to the system and removing heat from the slab, which was not insulated. Additionally, the calculations do not take into account heat losses that occur at the bottom of the slab. Only the temperature field on the upper surface of the plate was measured using a thermal imaging camera, assuming heat flow upwards. Even though the board is thermally insulated from the bottom, it is not perfect insulation. Heat losses from the bottom of the plate, estimated on the basis of the heat transfer coefficient up and down, were determined to be 4.9% in relation to the heat (heating power of the plate) that is given off by the upper surface of the plate. This is due to the polystyrene insulation, but it is not a perfectly insulated system.

At the start of the experiment, the initial room temperature was stabilized at $4 \text{ }^\circ\text{C}$. The parameters of the mock-up heating process were monitored using a Flir E30bx thermal camera with an accuracy of 0.1 K, an Airflow LCA301 thermal anemometer with an accuracy of 0.1 K and 0.05 m/s, and an on-wall room temperature sensor Auraton 2005 with an accuracy of 0.1 K.

The thermodynamic side of the process consists of two parts: heat transfer from the heated air on the internal pipe surface and heat transfer from the plate to the room. The fundamental parameter is the heating power of the plate. The methodology for its determination under natural convection assumptions is presented below. First, the Nusselt number Nu had to be determined by an equation [26]:

$$Nu = C \cdot (Gr \cdot Pr)^n \quad (1)$$

Depending on the product of the Grashof number and Prandtl number, values for the constants C and n used in calculations were determined according to Equation (1) based on the available literature data. It should be noted that the correlation of the Nusselt number may be a source of errors resulting from the determination of the Pr and Gr numbers, which in turn are closely related to the fluid parameters. These errors will be even greater when the fluid parameters are dynamically changed, which takes place at the beginning of the experiments in the heat transfer stabilization phase. When stable conditions are reached, for

which the efficiency of individual variants of the experiment was determined, Nu achieves statistically the highest accuracy throughout the entire experiment, which the authors are aware of. Therefore, the efficiency values are determined after heat transfer stabilization is achieved, where the dynamics of changes are the smallest.

On the definitional side, the Nusselt number facilitates the determination of the heat transfer coefficient α to the plate surface for the average temperature between the room and the plate temperature, measured as the mean value according to thermal imaging. Ultimately, the plate power q_p was determined using the equation:

$$dq_p = d\alpha \cdot dt_p, \text{ W/m}^2, \quad (2)$$

where dq_p is the unit power of the plate, W/m^2 and dt_p is the temperature difference between the plate temperature and the room temperature, K.

Another crucial piece of information necessary for plotting the temperature efficiency of the plate is the power supplied by the air stream, denoted as q_d .

$$dq_d = dv \cdot dc_p \cdot d\rho \cdot dt_d, \text{ W/m}^2, \quad (3)$$

where v is the airflow velocity through the channels, m/s ; c_p is the specific heat capacity of the air, kJ/kgK ; ρ is the density of the air, in kg/m^3 ; and dt_d is the temperature difference of the air between the inlet and outlet of the heating plate, K. The value of the heat supplied to the system, excluding heat losses to the pipes supplying heat to the heating plate, should in principle be the same as the power value of the fan heater, which had a power of 500 W during the experiment. Hence, the dq_d value can be treated with some approximation as the power of the electric heater.

Ultimately, the plate efficiency η_p is determined as the ratio of the obtained power dq_p to the supplied power dq_d :

$$\eta_p = dq_p/dq_d, \quad (4)$$

The Q_p and Q_d values refer to the amount of total heat per m^2 of the plate surface of the entire analyzed plate, unlike the unit values of q_p and q_d . The area of model A is $0.5 \times 2 \text{ m}$, i.e., 1 m^2 ; hence, the total heat values Q_d and Q_p are the same in value as the unit heat q_p and q_d . The tests were carried out according to the scheme shown in Figure 4. The measured values were the basis for determining the value of the Nu number and then the heat supplied by the heating plate to the Q_p environment. Taking into account the amount of heat supplied to the Q_d system by the fan heater, the heating efficiency of the plate was calculated. If the confidence resulting from the obtained results of the normal distribution was within the range of 7% (except for Variant 3, in which the highest confidence of 10% was obtained due to the variable physicochemical properties of the burned pellets and the smoke itself), difficult conditions were not analyzed during the experiment.

The experimental part was conducted in semi-industrial conditions to achieve stable measurement conditions, enclosed in a volume of 32.4 m^3 . The research was carried out for three variations of plate heating:

- Variant 1: Forced air surface heating without recirculation.
- Variant 2: Forced air surface heating with recirculation.
- Variant 3: Heating using flue gases from a pellet-fired boiler.

The layout of the mock-up is presented in Figures 5 and 6.

The connections at the inlet and outlet have been insulated with mineral wool and an aluminum foil layer.

The application of such a solution can find success in traditional construction with modern enhancements, paying homage to ancient engineering prowess. The integration of modern technology can breathe new life into age-old systems, showcasing their adaptability and potential for optimization without sacrificing the principles that have endured for centuries.

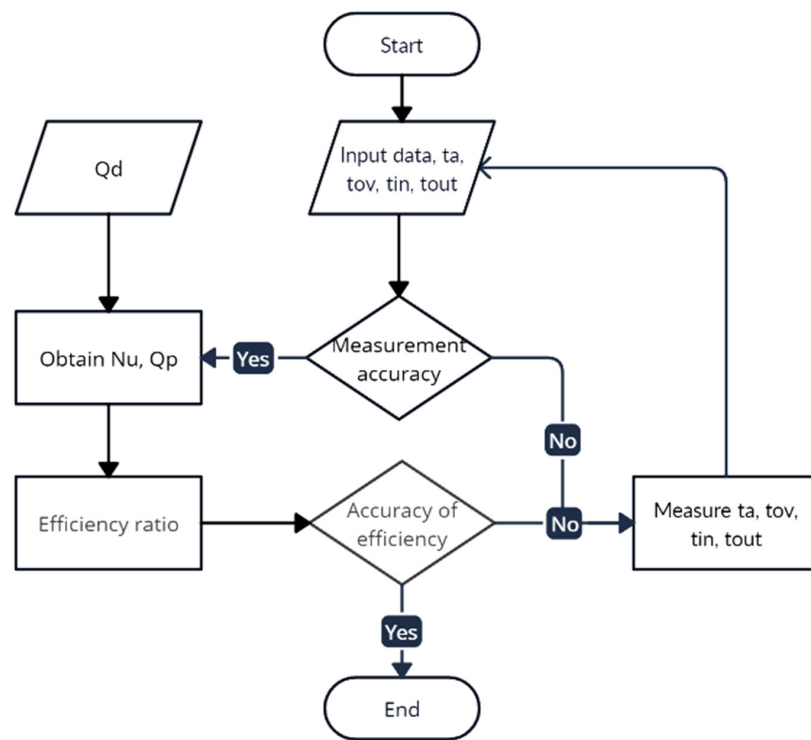


Figure 4. Flow chart of test measurements.



Figure 5. Layout and appearance of the mock-up.



Figure 6. Heating group: fan, electric heater, and connected temperature sensor (on the left); flow distribution manifold (on the right) (before insulation).

The advantages of the plate heating system are as follows:

1. Energy efficiency: The combination of a supply air heating system and panel heating systems enhances energy efficiency, leading to potential energy savings over time.
2. Flexible application: Particularly beneficial for intermittently used buildings, the system offers flexibility and adaptability in heating solutions for spaces like holiday cottages and banquet halls.
3. Improved thermal comfort: The ability to accumulate heat in external partitions contributes to improved thermal comfort within the building, creating a more pleasant environment.
4. Potential for heat recovery: The system allows for the effective recovery of heat generated from the heated fireplace enclosure, maximizing the utilization of energy resources.
5. Modernization of traditional systems: By incorporating modern technology into traditional heating systems, this approach revitalizes age-old methods, providing a balance between tradition and innovation.

The disadvantages of the plate heating system are as follows:

1. Complexity of implementation: Integrating multiple heating systems may introduce complexity in terms of installation, maintenance, and control, potentially requiring specialized knowledge.
2. Challenges with air recirculation: Implementing air recirculation, especially with pellet smoke, can pose distribution and mixing challenges, necessitating additional considerations and potential experimental studies.
3. Limited standalone efficiency: The panel heating system supplied with hot air is deemed as an auxiliary heating source due to relatively low efficiencies. It is not recommended as a standalone solution for primary heating in a building.
4. Economic considerations: The achieved low efficiencies in certain configurations may impact the economic feasibility of the system, potentially requiring it to be viewed as a supplementary solution rather than a cost-effective standalone option.
5. Dependency on heat source: The efficiency of the system is closely tied to the type of heat source and the heating medium it can supply within a given time unit, limiting its effectiveness based on the chosen components.

3. Results of the Study

The study investigated three distinct variants of surface heating systems, each employing different methods to achieve optimal thermal efficiency. Through comprehensive experiments and analyses, the research aimed to provide insights into the performance, advantages, and limitations of these heating configurations. The results offer a nuanced understanding of air surface heating without recirculation, air surface heating with recirculation, and air surface heating using smoke from pellet burning. The findings contribute valuable information for designing efficient and practical heating systems while recognizing the trade-offs inherent in each variant. This study serves as a foundation for informed decision making in the development and implementation of surface heating technologies.

3.1. Variant 1—Air Surface Heating without Recirculation

During the experiment, temperature changes in the plate surface were studied under various thermal load conditions. The heating element used in the study was heated air, and an electric heater was used to heat the air. In this way, the results related to the heating power of the plate and its basic parameters were obtained, allowing the determination of the efficiency of the entire surface heating system.

The experiment was conducted to determine whether the heat supplied with the appropriate parameters is capable of effectively heating the underfloor heating system to the point where it operates optimally.

The air heated by the electric heater flows through the plate, releases heat, and exits the room without recirculation. Measurements began when the ambient temperature and

the mock-up had the same temperature (winter period, 4 °C). The air used to heat the floor is drawn from outside the room, and the secondary air is discharged outside the room.

At the beginning of the measurements, the airflow parameters were determined, with a velocity of $v_p = 2.81$ m/s, and the diameter of the main duct was $d = 110$ mm. The measurements helped determine the airflow and the energy delivered to the air through the electric heater.

During the experiment, the room (walls, air) as well as the mock-up had a constant temperature of approximately 4 °C. The experiment lasted for 3.5 h, during which time the mock-up was heated from a temperature of 3.2 °C to a temperature of 17.1 °C. The temperature difference between the inlet and outlet air at the beginning of the measurement fluctuated at $\Delta t = 30$, and at the end of the study, it was already $\Delta t = 20$.

Figure 7 depict the heating of the mock-up of the experiment captured with a thermal imaging camera.

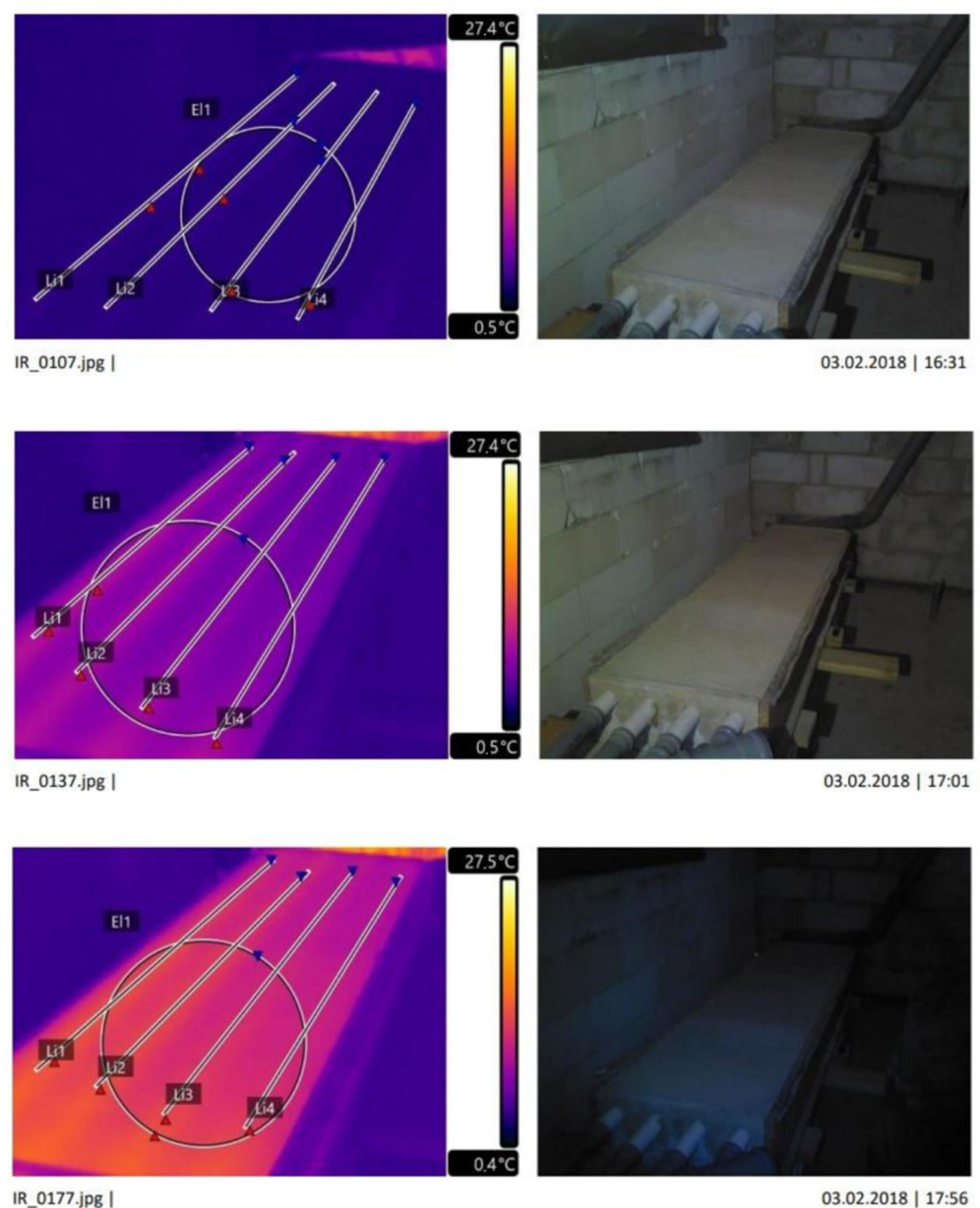


Figure 7. Heating of the mock-up at the 5th, 34th, and 89th minute of the experiment captured with a thermal imaging camera.

Based on the gathered data, a graph illustrating the temporal temperature distribution on the heating plate (lines L1–L4) and across the entire surface of the plate (E1) was created, as depicted in Figure 8.

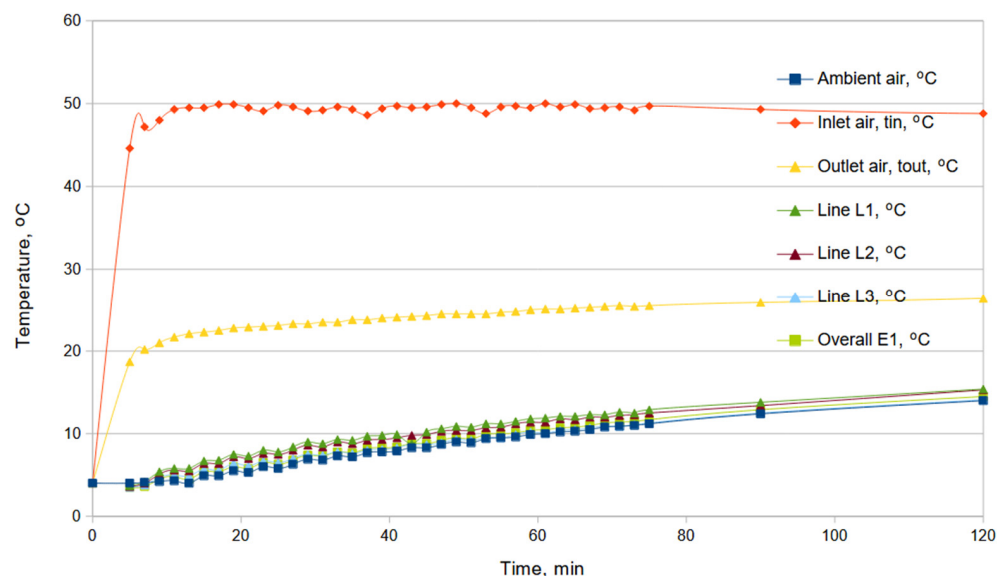


Figure 8. Temperature changes over time for the heated plate without recirculation.

Stable measurement conditions were achieved after approximately 15 min from the start of the measurement. The temperature profile aligns with expectations. A greater temperature difference between the air supplying the heating plate (tin) and the outlet air (tout) results in a more significant temperature increase in the ambient air. An increase in the plate temperature in an already heated room does not lead to significant temperature increases in the room.

In summary, for Variant 1, an experiment was conducted to examine temperature changes on the plate surface under various thermal load conditions. An electric heater was used to heat the air. The goal of the experiment was to assess whether the supplied heat with appropriate parameters could effectively warm the underfloor heating system to an optimal level. Over the course of the 3.5 h experiment, stable measurement conditions were achieved, and the mock-up temperature increased from 3.2 °C to 17.1 °C. The temperature difference between the inlet and outlet air, initially $\Delta t = 30$, decreased to $\Delta t = 20$ by the end of the study.

3.2. Variant 2—Air Surface Heating with Recirculation: Air Is Heated by an Electric Heater in a Closed-Loop System

Using recirculating air for the study involves connecting the hot air supply duct with the air manifold in a closed-loop system within the heated environment. In this cycle, an electric heater is still present. The main advantage of this solution is the heating balance, in which the electric heater is significantly less burdened because the air circulating in the system is only heated by a few degrees, while the energy used to heat the air is transferred directly to the heating plate.

Measurements commenced when the ambient temperature and the model's temperature were identical, both at 4 °C. Initially determined airflow parameters were $v_p = 2.81$ m/s, with a duct diameter of $d = 110$ mm. The measurements performed allowed for an accurate determination of the airflow and the energy delivered to the air by the electric heater. To establish the temperature distribution on the model's surface, a thermal imaging camera was employed.

The experiment lasted for almost 3 h. During this time, the model reached an average temperature close to 20 °C. The initial temperature of the room and the plate was very balanced, measuring 4.5 °C and 4.0 °C, respectively.

Figure 9 presents a graphical representation along with the degree of recirculation, which was manually adjusted when the heater's maximum temperature of 50 °C was reached. This allowed us to maintain a stable room temperature of 16.2 °C.

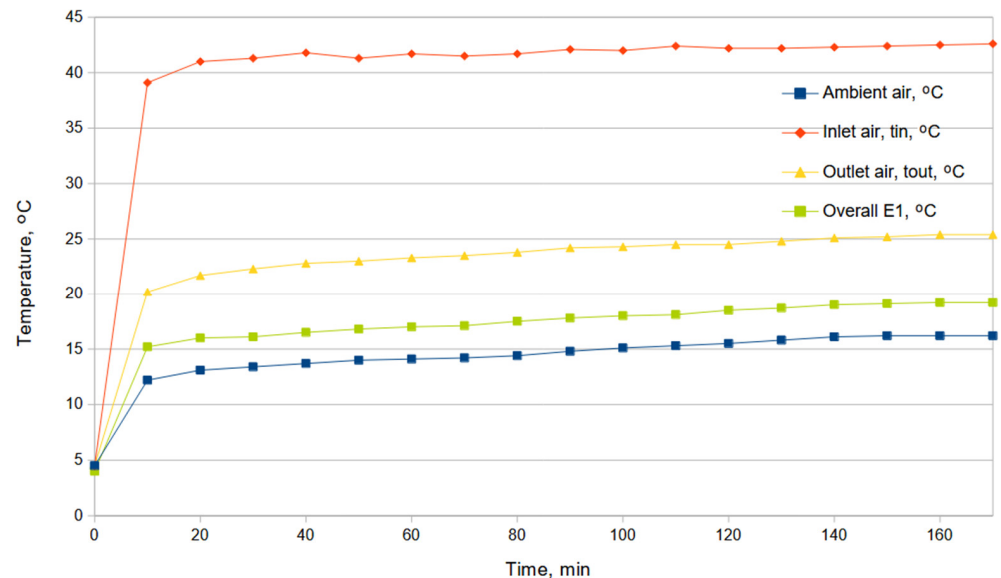


Figure 9. Temperature changes over time for the heated plate with recirculation: the air is heated by an electric heater in a closed-loop system.

Stable measurement conditions were achieved approximately 20 min after the start of the experiment. A portion of the heat required to warm the plate was obtained from the recirculation of the air leaving the plate. This was achieved by recirculating 100% of the air, which reduced the heat demand by lowering the inlet temperature to the heater by approximately 30% compared to Variant 1.

This chapter explores the use of recirculating air, connecting the hot air supply duct with the air manifold in a closed-loop system within a heated environment. An electric heater is employed in this cycle. The key advantage of this approach lies in maintaining thermal balance, as the electric heater is less burdened when the circulating air is only heated by a few degrees, and the energy used for heating the air is directly transferred to the heating plate. The experiment, lasting nearly 3 h, resulted in an average model temperature reaching close to 20 °C. Stable measurement conditions were achieved approximately 20 min after the experiment began, and air recirculation reduced the heat demand by about 30%.

3.3. Variant 3—Air Surface Heating without Recirculation: The Source of Heat Is the Smoke Generated from Burning Pellets in the Fireplace

The study lasted for over an hour. After this time, a temperature of 8.1 °C was achieved on the heated surface, starting from 2.3 °C, although the highest recorded temperature reached 13.8 °C.

The heating of the model involved passing a stream of pellet smoke generated by the fireplace through a collector submerged in the screed. The device was placed outside the room where the test model was located to minimize heat losses from the heat source. The thermal energy typically removed with pellet smoke could be utilized for heating in this way. In a different scenario, such a system would provide immense benefits. Assuming that our room is heated by warm air, we can lower the inlet temperature. The air, first passing through the surfaces of the room, warming them, would then enter the same room

at a cooler temperature, contributing to maintaining the room's thermal comfort. Figure 10 presents the temperature changes for the analyzed variant.

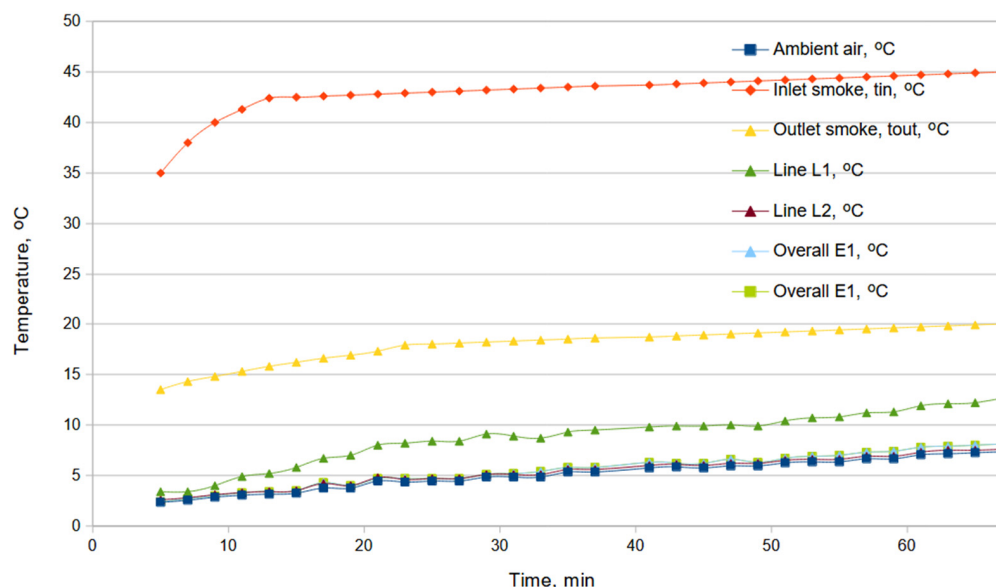


Figure 10. Temperature changes over time for the heated plate with recirculation: the source of heat is the smoke generated from burning pellets in the fireplace.

Due to the lower smoke temperature compared to the air temperature obtained with an electric heater, a longer heating period and stabilization time are observed. This is the weakest solution among those analyzed, possibly due to the low smoke temperature obtained from the pellets. In the case of more calorific fuel, this would be one of the better solutions, historically used due to the higher density and heat capacity of the smoke, but it can be inconvenient due to its sootiness.

The flow speeds through the model were kept constant by a nonadjustable fan installed in the system, adjusted to the expected actual speeds in the channels, which are the resultant between the flow resistance and the heat transfer coefficient. Therefore, the influence of flow speed on the obtained values is relatively small due to its very small fluctuations.

The data obtained during the experiments were used to determine both the power delivered to the system and the power acquired from the heating plate. In the calculations, the aspect of thermal radiation was not taken into account. Based on the room temperature and the average temperature of the heating plate, the heating power of the plate (Q_p , according to 2) and the power delivered to the plate through hot air (Q_d , according to 3) were determined. To accomplish this, a series of necessary parameters and dimensionless numbers were calculated to determine the convective heat transfer coefficient (α) resulting from natural convection (heat exchange by convection). Table 2 presents an example based on Variant 1, i.e., the heating plate being supplied with hot air in an open circuit without recirculation, presenting the power obtained from the heating plate (Q_p). It was assumed that certain quantities would be constant within this temperature range, such as dynamic viscosity (1.73×10^{-5} Pas), specific heat capacity of air (1005 J/kgK), thermal conductivity of air (0.0246 W/mK), and Prandtl number ($Pr = 0.707$), while the other values are listed in Table 2.

Table 2. Summary of results for Variant 1 to determine the heating power of the plate Qp.

ta, °C	tov, °C	$\Delta t = t_{ov} - t_a$, K	Gr × Pr	Nusselt No. Nu	α , W/m ² K	Qp, W
4.1	4.5	0.4	7,747,107	28.49	1.402	56.07
4.4	4.8	0.4	7,738,739	28.48	1.401	56.05
4.1	4.5	0.4	7,747,107	28.49	1.402	56.07
5	5.4	0.4	7,722,057	28.47	1.401	56.02
5	5.4	0.4	7,722,057	28.47	1.401	56.02
5.5	6	0.5	9,633,535	30.08	1.48	74.01
5.3	5.8	0.5	9,640,449	30.09	1.48	74.02
6	6.5	0.5	9,616,295	30.07	1.479	73.97
5.8	6.3	0.5	9,623,184	30.08	1.48	73.99
6.3	6.8	0.5	9,605,981	30.06	1.479	73.95
6.9	7.4	0.5	9,585,418	30.05	1.478	73.91
6.9	7.3	0.4	7,669,702	28.42	1.398	55.93
7.3	7.8	0.5	9,571,758	30.04	1.478	73.89
7.3	7.7	0.4	7,658,771	28.41	1.398	55.91
7.7	8.2	0.5	9,558,137	30.03	1.477	73.86
7.8	8.3	0.5	9,554,738	30.02	1.477	73.86
7.9	8.4	0.5	9,551,341	30.02	1.477	73.85
8.3	8.8	0.5	9,537,778	30.01	1.476	73.82
8.3	8.8	0.5	9,537,778	30.01	1.476	73.82
8.7	9.2	0.5	9,524,254	30	1.476	73.8

In this variant, only slightly more than 100 W of heat was obtained in the heating plate. Meanwhile, the amount of heat delivered to the system is presented in Table 3. It was assumed here that the diameter of the heat distribution pipes inside the plate was 110 mm, there were four pipes, the constant flow velocity was 2.81 m/s, and the average air density was 1.165 kg/m³.

Table 3. Summary of results for Variant 1 to determine the heating power of the plate Qd and efficiency.

tin, °C	tout, °C	Volume Flow V, m ³ /s	Qd, W	η_p , %
48.0	21.0	0.106817	500.0	11.2
49.3	21.7	0.106817	500.0	11.2
49.5	22.1	0.106817	500.0	11.2
49.5	22.3	0.106817	500.0	11.2
49.9	22.5	0.106817	500.0	11.2
49.9	22.8	0.106817	500.0	14.8
49.5	22.9	0.106817	500.0	14.8
49.1	23.0	0.106817	500.0	14.8
49.8	23.1	0.106817	500.0	14.8
49.6	23.3	0.106817	500.0	14.8
49.1	23.3	0.106817	500.0	14.8
49.2	23.5	0.106817	500.0	11.2
49.6	23.5	0.106817	500.0	14.8
49.3	23.8	0.106817	500.0	11.2
48.6	23.8	0.106817	500.0	14.8
49.1	23.9	0.106817	500.0	14.8
49.7	24.1	0.106817	500.0	14.8
49.5	24.2	0.106817	500.0	14.8
49.6	24.3	0.106817	500.0	14.8
49.9	24.5	0.106817	500.0	14.8

The standard deviation for the normal distribution and the confidence for all variants are presented in Table 4.

Table 4. Standard deviation for the normal distribution and the confidence for all variants.

Variant	Average Efficiency, %	Standard Deviation	Confidence Interval, %	Confidence
1	15.8	2.51	5	0.0492
2	21.6	1.53	5	0.0299
3	30.9	6.34	10	0.1043

The average thermal efficiency for Variant 1 is approximately 15.8% with a standard deviation of 2.51. For Variant 2, the average thermal efficiency is 21.6% with a standard deviation of 1.53. In the case of Variant 3, the thermal efficiency of the heating plate is 30.9% with a standard deviation of 6.34. This is the best variant, as expected due to the higher density and heat capacity of the smoke. However, it is a debatable solution due to the possibility of smoke penetration into the room, which significantly limits the use of smoke for heating using the presented heating plate.

4. Conclusions

The integration of supply air heating with panel heating systems offers advantages, particularly in intermittently used buildings where constant supervision is difficult. This approach is beneficial in places where water-based heating systems are not feasible. Accumulating heat in external partitions enhances thermal comfort and energy efficiency, especially with continuous heating. The study evaluates three heating variants: air surface heating without recirculation, with recirculation, and utilizing pellet smoke. Each variant has advantages and challenges, contributing valuable insights for designing efficient heating systems. Considerations include recirculation, alternative heat sources, and practical limitations. While the integrated system improves energy efficiency and comfort, complexity and economic viability must be considered. The study proposes novel approaches, explores interactions between heating methods, and draws inspiration from ancient Roman hypocaustum systems. Experimental setups and detailed methods provide insights into heating capacity, thermal load conditions, and efficiency determinations. The manuscript addresses energy efficiency in older buildings with air heating systems, proposing new assessment methods using heated air.

Author Contributions: Conceptualization, S.R. and K.N.; methodology, S.R. and K.N.; formal analysis, S.R. and K.N.; resources, S.R. and K.N.; writing—original draft preparation, S.R. and K.N.; writing—review and editing, S.R. and K.N. All authors have read and agreed to the published version of the manuscript.

Funding: This research received no external funding.

Data Availability Statement: The original contributions presented in the study are included in the article, further inquiries can be directed to the corresponding author.

Conflicts of Interest: The authors declare no conflict of interest.

References

- Martínez-Molina, A.; Tort-Ausina, I.; Cho, S.; Vivancos, J.-L. Energy Efficiency and Thermal Comfort in Historic Buildings: A Review. *Renew. Sustain. Energy Rev.* **2016**, *61*, 70–85. [[CrossRef](#)]
- Pruitt, L.N.D.; Kramer, S.W. How Historical Solutions to Thermal Comfort Influenced Modern Construction Efforts. *Procedia Eng.* **2017**, *196*, 880–887. [[CrossRef](#)]
- Liu, W. The Evolution of Cold Adaptation Technology within Ancient Buildings in Amur River Basin Viewed from Archaeology. *Int. J. Environ. Res. Public Health* **2022**, *19*, 14470. [[CrossRef](#)]
- Barba, S.; Citarella, M.C.; d’Ambrosio Alfano, F.R.; D’Andria, G.; Danzi, M.; Donciglio, E.; Palella, B.I. The Heating System of the Piccole Terme in Baia: Some Hypotheses. *Measurement* **2018**, *118*, 387–397. [[CrossRef](#)]
- Bansal, N.K. India Characteristic Parameters of a Hypocaust Construction. *Build. Environ.* **1998**, *34*, 305–318. [[CrossRef](#)]
- Shemesh, A.O. “He Who Enters the Bath-House Utters Two Blessings”: On the Evolvement and Decline of an Ancient Jewish Prayer. *Religions* **2017**, *8*, 225. [[CrossRef](#)]

7. Theis, C. Saving Energy in Old Buildings. In *Passive and Low Energy Alternatives I*; Bowen, A., Vagner, R., Eds.; Pergamon: Oxford, UK, 1982; pp. 5-1–5-8, ISBN 978-0-08-029405-6.
8. Lidelöw, S.; Örn, T.; Luciani, A.; Rizzo, A. Energy-Efficiency Measures for Heritage Buildings: A Literature Review. *Sustain. Cities Soc.* **2019**, *45*, 231–242. [[CrossRef](#)]
9. Martínez-Garrido, M.I.; Aparicio, S.; Fort, R.; Anaya, J.J.; Izquierdo, M.A.G. Effect of Solar Radiation and Humidity on the Inner Core of Walls in Historic Buildings. *Constr. Build. Mater.* **2014**, *51*, 383–394. [[CrossRef](#)]
10. Gagliano, A.; Liuzzo, M.; Margani, G.; Pettinato, W. Thermo-Hygrometric Behaviour of Roman Thermal Buildings: The “Indirizzo” Baths of Catania (Sicily). *Energy Build.* **2017**, *138*, 704–715. [[CrossRef](#)]
11. Basaran, T.; Ilken, Z. Thermal Analysis of the Heating System of the Small Bath in Ancient Phaselis. *Energy Build.* **1998**, *27*, 1–11. [[CrossRef](#)]
12. Korkina, E.V.; Gorbarenko, E.V.; Voitovich, E.V.; Tyulenev, M.D.; Kozhukhova, N.I. Temperature Evaluation of a Building Facade with a Thin Plaster Layer under Various Degrees of Cloudiness. *Energies* **2023**, *16*, 5783. [[CrossRef](#)]
13. Cabeza, L.F.; de Gracia, A.; Pisello, A.L. Integration of Renewable Technologies in Historical and Heritage Buildings: A Review. *Energy Build.* **2018**, *177*, 96–111. [[CrossRef](#)]
14. Hesarakı, A.; Huda, N. A Comparative Review on the Application of Radiant Low-Temperature Heating and High-Temperature Cooling for Energy, Thermal Comfort, Indoor Air Quality, Design and Control. *Sustain. Energy Technol. Assess.* **2022**, *49*, 101661. [[CrossRef](#)]
15. Nowak, K. Heating of External Surfaces by Means of Heat Pumps. *E3S Web Conf.* **2018**, *44*, 00128. [[CrossRef](#)]
16. Gruber, S.; Rola, K.; Urbancl, D.; Goričanec, D. Carbon-Free Heat Production for High-Temperature Heating Systems. *Sustainability* **2023**, *15*, 15063. [[CrossRef](#)]
17. Rakesh, C.; Vivek, T.; Balaji, K. Experimental Investigation on Cooling Surface Heat Transfer Behavior of a Thermally Activated Building System in Warm and Humid Zones. *Case Stud. Therm. Eng.* **2023**, *49*, 103254. [[CrossRef](#)]
18. Kim, M.K.; Liu, J.; Cao, S.-J. Energy Analysis of a Hybrid Radiant Cooling System under Hot and Humid Climates: A Case Study at Shanghai in China. *Build. Environ.* **2018**, *137*, 208–214. [[CrossRef](#)]
19. Ma, Z.; Awan, M.B.; Lu, M.; Li, S.; Aziz, M.S.; Zhou, X.; Du, H.; Sha, X.; Li, Y. An Overview of Emerging and Sustainable Technologies for Increased Energy Efficiency and Carbon Emission Mitigation in Buildings. *Buildings* **2023**, *13*, 2658. [[CrossRef](#)]
20. Basolo, V.; Strong, D. Understanding the Neighborhood: From Residents’ Perceptions and Needs to Action. *Hous. Policy Debate* **2002**, *13*, 83–105. [[CrossRef](#)]
21. Boussaa, Y.; Doodoo, A.; Nguyen, T.; Rupa-Gadd, K. Integrating Passive Energy Efficient Measures to the Building Envelope of a Multi-Apartment Building in Sweden: Analysis of Final Energy Savings and Cost Effectiveness. *Buildings* **2023**, *13*, 2654. [[CrossRef](#)]
22. Sun, J.; Ren, Z.; Guo, J. Mechanical Ventilation Heat Recovery Modelling for AccuRate Home—A Benchmark Tool for Whole House Energy Rating in Australia. *Energies* **2023**, *16*, 6801. [[CrossRef](#)]
23. Chen, C. Searching for Intellectual Turning Points: Progressive Knowledge Domain Visualization. *Proc. Natl. Acad. Sci. USA* **2004**, *101* (Suppl. S1), 5303–5310. [[CrossRef](#)] [[PubMed](#)]
24. Chen, C.; Leydesdorff, L. Patterns of Connections and Movements in Dual-Map Overlays: A New Method of Publication Portfolio Analysis. *J. Assoc. Inf. Sci. Technol.* **2014**, *65*, 334–351. [[CrossRef](#)]
25. Kut, P.; Pietrucha-Urbanik, K. Most Searched Topics in the Scientific Literature on Failures in Photovoltaic Installations. *Energies* **2022**, *15*, 8108. [[CrossRef](#)]
26. Hong, J.; Wang, Z.; Li, J.; Xu, Y.; Xin, H. Effect of Interface Structure and Behavior on the Fluid Flow Characteristics and Phase Interaction in the Petroleum Industry: State of the Art Review and Outlook. *Energy Fuels* **2023**, *37*, 9914–9937. [[CrossRef](#)]

Disclaimer/Publisher’s Note: The statements, opinions and data contained in all publications are solely those of the individual author(s) and contributor(s) and not of MDPI and/or the editor(s). MDPI and/or the editor(s) disclaim responsibility for any injury to people or property resulting from any ideas, methods, instructions or products referred to in the content.